A Stretchable Capacitive Strain Sensor Having Adjustable Elastic Modulus Capability for Wide-Range Force Detection

Peng-Juan Cao, Yiwei Liu,* Waqas Asghar, Chao Hu, Fali Li, Yuanzhao Wu, Yunyao Li, Zhe Yu, Shengbin Li, Jie Shang, Xincai Liu,* and Run-Wei Li*

Stretchable strain sensors are important components of soft robotics, rehabilitation assistance, and human health monitoring systems. However, strain sensors capable of wide-range force detection with adjustable modulus facilities are highly desirable to obtain mechanical feedback in various scenarios. Herein, a stretchable capacitive strain sensor capable of adjustable modulus and wide-range force detection is reported. The sensor consists of two liquid metals (LMs) filled thermoplastic elastomer (TPE) tubes encapsulated in flexible silicone. The adjustable modulus capability of the sensor is attained by mounting the sensor with springs of different elastic coefficients. During electromechanical tests, the elastic coefficient-dependent adjustable modulus is obtained in the range of 0.78–10.3 MPa. After optimizing the performance, a sensor capable of wide force-sensing range (0.07–74 N), high cyclic stability (>3500 cycles), with low hysteresis, good linearity, and fast response time (<50 ms) is achieved. Finally, a digital display system is developed to display the amount of detected force during the loading of the sensor, which confirms the great capability of the sensor to be applied in joint rehabilitation and soft robotic fields.

1. Introduction

Stretchable strain sensors are widely used to obtain mechanical feedback from the soft interfaces of various fields: health care, rehabilitation monitoring, human–machine interaction, soft robotics, and mass measurement.[1–11] Generally, these sensors are used to measure large strains (>2%) of objects.[12–14] During stretching, force applied on sensor interacts with produced strain, and it is necessary to measure the exact value of the interacting force like in the case of joint bending.[15,16] Wide-range force detection sensors are crucial for soft robots lifting variable loads and rehabilitation training of patients having broken joints.[17–19] Therefore, it is crucial to develop strain sensors capable of wide-range force detection, without showing any failure at large loads. The sensor's force bearing capability directly depends on its modulus.[20–22] Wide-range force detection can be attained easily by simply regulating the elastic modulus of the sensor.

To attain adjustable modulus, various promising methods are reported in the literature: structural design,[21–26] designing of composite materials,[27,28] and chemical synthesis method.[29] Maziz et al. and Kharkova et al. used a structural design method based on weaving and knitting and obtained adjustable modulus strain sensors made up of electroactive polymers.[30,31] Jang et al. achieved adjustable modulus by using a low-modulus matrix structurally reinforced with an open, stretchable network of hard and soft structural composites.[27] Both researchers have achieved the adjustable modulus in the range of 0.8–4 MPa. Dickey et al. used the composite materials design method and realized an adjustable modulus from 0.6 to 5 MPa by developing metamaterial-like core–shell fibers. The liquid metal (LM) core of these fibers broke continuously with the increasing of applied stress and the load-bearing capacity of those fibers did not exceed 7 N.[28] Furthermore, Dong et al. obtained an adjustable elastic modulus from 0.08 to 45.6 MPa, by using double physical cross-linked hydrogel (DP gel), developed by a

P.-J. Cao, Prof. X. Liu
School of Material Chemistry
Ningbo University
Ningbo, Zhejiang 315201, P. R. China
E-mail: xincailiu@nbu.edu.cn

P.-J. Cao, Prof. Y. Liu, W. Asghar, C. Hu, F. Li, Y. Wu, Y. Li, Z. Yu, S. Li, Prof. J. Shang, Prof. R.-W. Li
CAS Key Laboratory of Magnetic Materials and Devices
Ningbo Institute of Materials Technology and Engineering
Chinese Academy of Sciences
Ningbo 315201, P. R. China
E-mail: liuyw@nimte.ac.cn; runweili@nimte.ac.cn

The ORCID identification number(s) for the author(s) of this article can be found under https://doi.org/10.1002/adem.201901239.

DOI: 10.1002/adem.201901239

Prof. Y. Liu, Prof. J. Shang, Prof. R.-W. Li
College of Materials Science and Opto-Electronic Technology
School of Future Technology
University of Chinese Academy of Sciences
Beijing 100049, P. R. China

P.-J. Cao, Prof. Y. Liu, W. Asghar, C. Hu, F. Li, Y. Wu, Y. Li, Z. Yu, S. Li, Prof. J. Shang, Prof. R.-W. Li
Zhejiang Province Key Laboratory of Magnetic Materials and Application Technology
Ningbo Institute of Materials Technology and Engineering
Chinese Academy of Sciences
Ningbo 315201, P. R. China

Y. Li
College of Information Engineering
Nanjing University of Finance and Economics
Nanjing 210046, P. R. China

chemical synthesis method.[29] All of these methods are suitable for manufacturing adjustable modulus materials, but these methods cannot be used to manufacture adjustable modulus strain sensors. In addition to this, a lot of methods are available for micro-force sensing, but measuring larger loads still remains a significant challenge due to the fix and low modulus of the sensor.

Herein, we report a stretchable capacitive strain sensor, which is capable of adjustable modulus and wide-range force detection. The sensor consists of two thermoplastic elastomer (TPE) tubes encapsulated in flexible silicone. The core of TPE tubes is filled with LM which serves as electrodes. LM is selected as a conductive material because of its high electrical conductivity at large strains.[32] In addition, conventional springs of the different elastic coefficients are mounted with a sensor to adjust its modulus on demand and make it capable of wide-range force detection. During electromechanical tests, the adjustable modulus is obtained in the range of 0.78–10.3 MPa. By combining the aforementioned parameters, a sensor capable of wide force-sensing range (0.07–74 N), with low hysteresis, good linearity, and fast response time (<50 ms) are obtained. Our sensor is found highly robust, which bears a good repeatable response when stretched and relaxed for over 3500 cycles. Finally, we developed a digital display system, which displays the amount of detected force during the loading of the sensor, and confirms the capability of the sensor to be applied in joint rehabilitation and soft robotics.

2. Results and Discussion

2.1. Operating Principle and Fabrication of Strain Sensor

Figure 1a shows the fabrication steps and working mechanism of the capacitive strain sensor with adjustable elastic modulus. Sensor electrodes consist of two TPE tubes (1.5 mm inner diameter, 2 mm outer diameter, 50 mm length) injected with LM. Finally, a tubular-like strain sensor is obtained by encapsulating these electrodes in flexible silicone. Detailed manufacturing steps of sensor are presented in Section 4 (Figure S1, Supporting Information). When the sensor is subjected to stretching strain, its capacitance changes similar to that of the ideal parallel plate capacitor (Figure 1a (i)), the length of the sensor increases while its width and thickness decrease during stretching strain. As a result, the distance between the two electrodes decreases according to the Poisson effect, which leads to a rise in the total capacitance of the sensor. However, TPE tubes exhibit low Young's modulus, which leads to the mechanical failure of
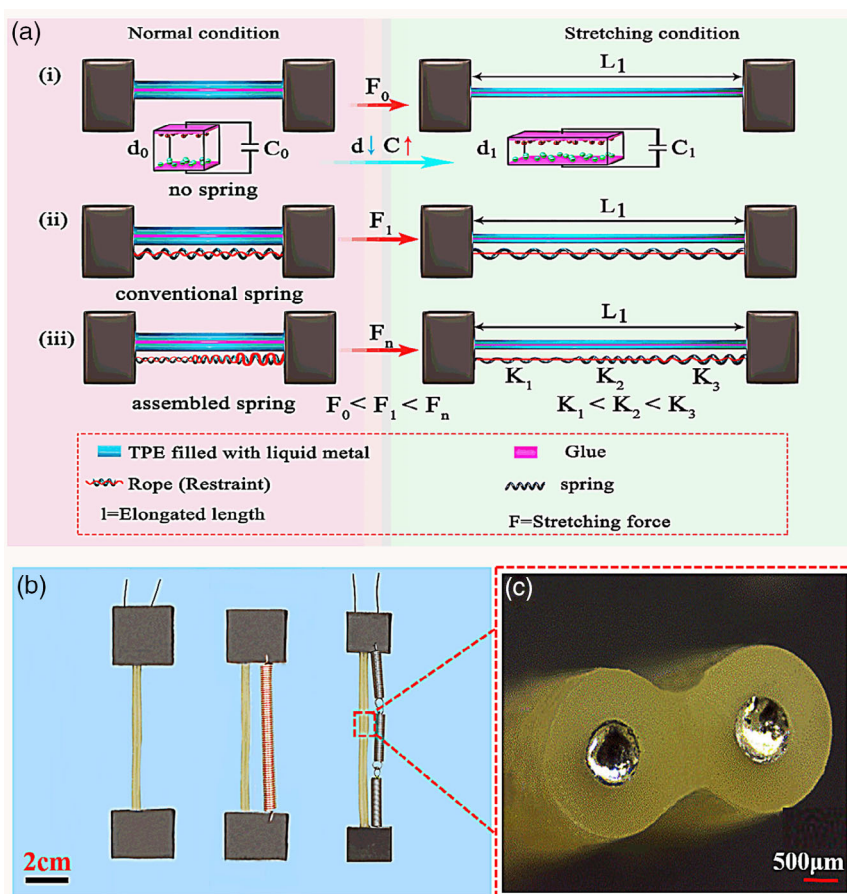

Figure 1. Working mechanism of capacitive strain sensor with adjustable modulus capability. a) Work mechanism of strain sensor during normal and stretching conditions. b) Image showing the normal strain sensor (left), the conventional spring-mounted strain sensor (center), and strain sensor mounted with the assembled spring (right). c) Optical microscopic image of LM-filled TPE tubes, which confirms the uniform filling of LM.

the sensor at certain stretching force F_0 and limits the detection range of the sensor to elongated length L_1. So, it is necessary to adjust the load-carrying capacity of the sensor by tuning its elastic modulus.

Conventional springs with spiral structure exhibit good tensile properties, which directly depend on their elastic coefficient. By changing the spring's elastic coefficient, we can easily adjust the modulus of conventional springs within their elastic deformation range. If spring is mounted with the strain sensor, it will share the load of the sensor during stretching and enables it to withstand larger load F_1 under the same elongated length, L_1 (Figure 1a (ii)). The geometry of our sensor is highly suitable for placing it either in parallel or in the center of the spring, to form a complete device. If an assembled spring is prepared by combining springs of different elastic coefficients and attached with the sensor, it will enable the sensor to bear a larger stretching force (F_n) with the same elongation L_1 (Figure 1a (iii)). Using conventional and assembled spring enable sensor to withstand larger force as compared with normal sensor, but elongation of sensor will remain intact. In this way, sensor's force detection range increases while maintaining its adjustable modulus capability. If conventional spring is attached to the sensor, adjustable modulus can be attained by changing the spring every time while using an assembled spring solves this problem. In this research, we have used this assembled spring only for the application demo of our sensor, remaining characterization is conducted by using various conventional springs. Figure 1b shows the images of a capacitive strain sensor (left), a conventional spring-mounted strain sensor (center), and strain sensor mounted with the assembled spring (right). The microscopic image of the sensor's cross section confirms that LM has efficiently filled the core of two TPE tubes (Figure 1c).

2.2. Mechanical Properties of Strain Sensors

Increasing the elastic coefficient of spring also affects their elasticity. To investigate the effect of spring elastic coefficient on modulus and tensile properties of the capacitive strain sensor, three different spring-mounted strain sensors were prepared. These sensors are designated as k_1, k_2, and k_3 mounted with springs of different elastic coefficients ($K_1 = 6.92$ g mm^{-1}, $K_2 = 36.71$ g mm^{-1}, $K_3 = 175$ g mm^{-1}). Capacitive strain sensor with no spring is designated as k_0.

Figure 2a shows the stress–strain curves of sensors: k_0, k_1, k_2, and k_3. The elastic modulus of the sensors is evaluated from the slope of stress–strain curves. The stress–strain curve of k_0 exhibits the smallest slope, whereas the slope of other curves increases with the increase in spring elastic coefficients. In other words, the sensor modulus increased from 0.78 to 10.3 MPa, with the increase in spring elastic coefficients. When the elastic coefficient is >175 g mm^{-1}, stretching the spring beyond 100% becomes difficult. Figure 2b shows the mechanical performance of sensors under the constant load of 4 N. Sensors are stretched under the same applied load, but they have shown different elongations of 100%, 40%, 12%, and 4%, respectively.

The effect of adjustable modulus on the elongation of sensors is demonstrated by applying a load of 400 g on the sensors (Figure 2c). The initial length of all the sensors is L. When the load is applied on k_0, k_1, k_2, and k_3 sensors, they have shown elongations of ΔL_0, ΔL_2, ΔL_3, and ΔL_4, respectively. The sensor
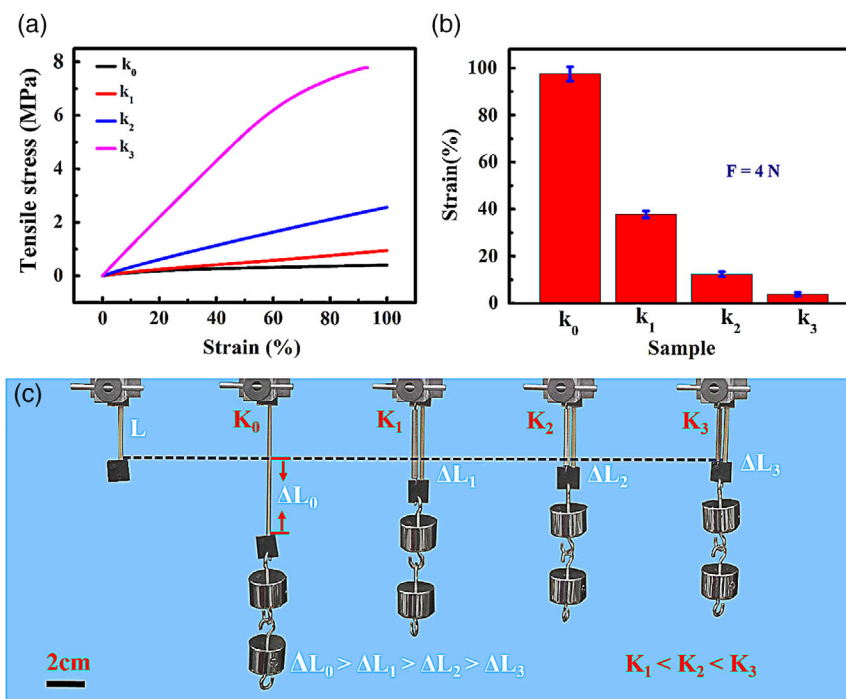

Figure 2. Mechanical properties of the normal and spring-mounted strain sensors. a) The stress–strain curves of strain sensors determined at a strain rate of 10 mm min^{-1}. k_0 corresponds to normal strain sensor, and k_1, k_2 and k_3 correspond to spring-mounted sensors with different elastic coefficients. b) Strain variation of sensors evaluated at the loading force of 4 N. c) Different elongations produced in sensors under an applied load of 400 g.

ADVANCED
SCIENCE NEWS

www.advancedsciencenews.com

ADVANCED
ENGINEERING
MATERIALS

www.aem-journal.com

k_0 has shown maximum elongation, whereas the elongation decreases with the increase in the elastic coefficient of spring. Overall observed pattern of samples' elongation is $\Delta L_0 > \Delta L_1 > \Delta L_2 > \Delta L_3$. Figure 2c confirms that the elongation of sensors decreases with the increase in sensors' modulus, which confirms the enhancement of the load-bearing capacity of the sensor, i.e., k_3 elongates lesser than k_1 while bearing the same amount of load.

2.3. Electrical Characterization of Strain Sensors

The electromechanical characterization of strain sensors is shown in **Figure 3**. Figure 3a shows the capacitive response of k_0 and k_1 sensors when they are subjected to the repeated stretching strain of 100%. The relative capacitance of sensors increases with the increase in applied strain. k_1 has shown a linear response, which fits well with the fitted line. The performance of both sensors under the loading and unloading phase coincides with each other ($R^2 = 0.99992$), which confirms that spring has not disturbed the electromechanical performance of the sensor. Moreover, the slope of both capacitance curves differed only by $<0.008\%$, which confirms the occurrence of no hysteresis. This confirms that other springs (k_1 and $k_{2)}$ will also not impair the electromechanical performance of the sensor.

Relative change of capacitance with respect to applied load is shown in Figure 3b. The load-carrying capacity of sensors increases with the increase in modulus of the sensors. When the value of $\Delta C/C(\%) = 4.0$, k_3 as shown a ten times increase in load-carrying capacity as compared with k_1. More importantly, the maximum load detection limit increases rapidly with the
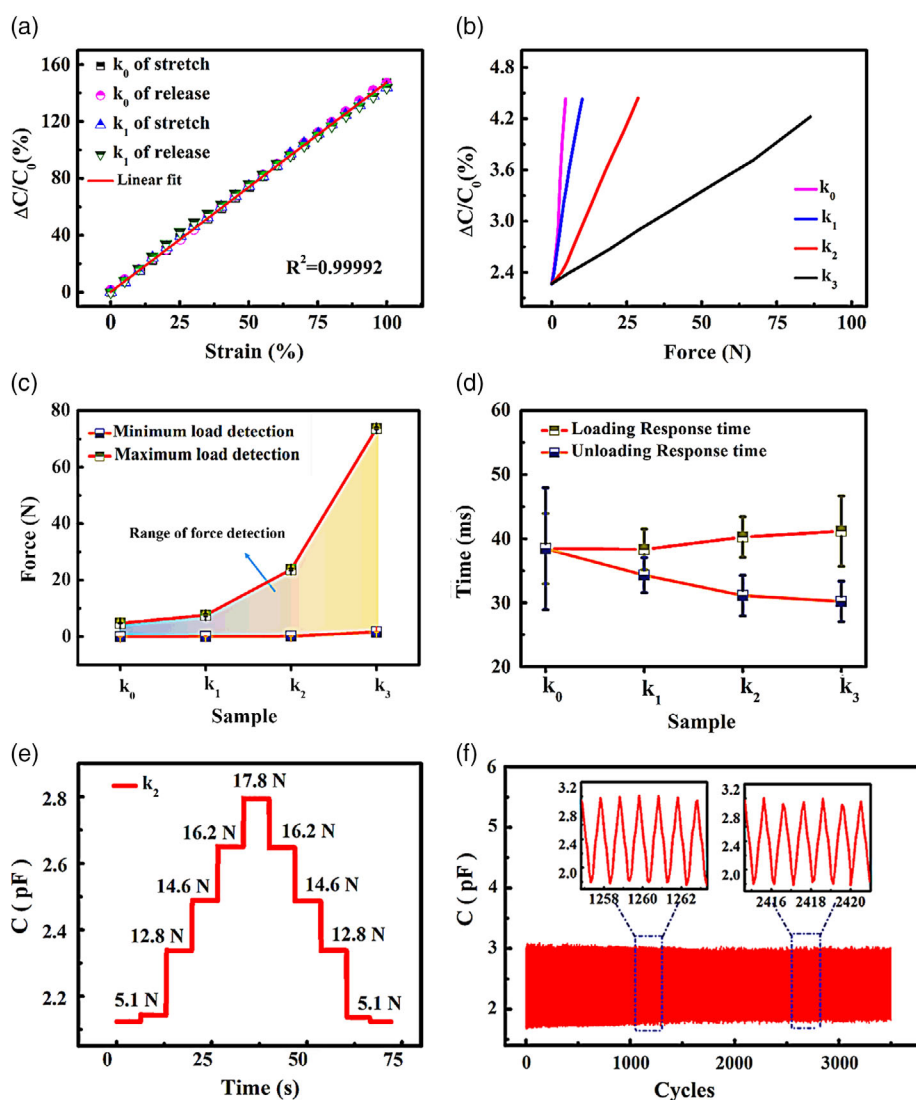

Figure 3. Electromechanical characterization of strain sensors. Strain-sensing properties of the capacitive strain sensor. a) Relative change in capacitance of sensors with respect to the repeated strain of 100%. b) Relative capacitance changes of the sensors as a function of applied force. c) Minimum and maximum detection limit of sensors. d) The response time of sensors determined at a strain of 0.2% at the rate of 42.5 mm s^{-1}. e) Capacitance signals at various repeated stresses indicating good repeatability of the sensor k_2. f) The stability of the sensor tested for 3500 cycles under an applied strain of 50% and the insets show the detailed capacitance signals under a different number of cycles.

increase in modulus, whereas no significant change occurred in the minimum load detection limit (Figure 3c). As a result, broad load detection range from 0.07 to 74 N is obtained by just mounting the sensor with spring of larger elastic modulus.

Response time and recovery time of the capacitive strain sensor are evaluated by applying a strain of 0.2% and at the rate of 42.5 mm s^{-1}. Figure 3d shows that loading response time initially decreases, then increases progressively with the increase in modulus of spring. While unloading response time decreases constantly with the increase in modulus. Overall, the sensor presented a fast response time of <50 ms during loading and unloading response time of ≈35 ms. The difference in the loading and unloading response time has occurred because unloading is slower than loading. During loading, response time decreases initially because k_1 is a spring-mounted sensor, the presence of spring is responsible for this decrease.

Furthermore, we investigated the repeatability of k_1, k_2, k_3 applying variable loads at a speed of 25 mm s^{-1} and holding time of 10 s. Repeatability of k_2, k_1, and k_3 is shown in Figure 3e and Figure S2, Supporting Information, which confirms that that the spring-mounted sensor exhibits stable response with high repeatability. Mechanical robustness of k_1. is tested by applying a repeated strain of 50% (rate = 5.7 mm s^{-1}). Figure 3f confirms that our sensor endured 3500 loading–unloading cycles without showing any obvious fatigue. Insets of Figure 3f show that the capacitance signal keeps its amplitude and waveform at different stages of the test, confirming the high stability of the device. Performance comparison of the current sensor with previously published literature is shown in Table S1, Supporting Information, which depicts that our sensor exhibits good performance in terms of wide-range force detection and linearity.[33–38]

2.4. The Intelligent Weight Measuring System

Figure 4 shows the application demo of our sensor. As our sensor exhibits a strain-dependent capacitance response, so it can be used as a transducer for soft robotics. Our device is capable of attaining adjustable modulus, but it can be done in a more efficient way by changing conventional spring to the assembled spring. Conventional spring exhibits fix modulus, but the assembled springs exhibit adjustable modulus and relatively high load-bearing capacity. Also, the load-bearing capacity of the assembled spring is greater than the conventional spring. For this purpose, three springs having elastic coefficients k_1, k_2, k_3 are attached with each other to obtain an assembled spring followed by mounting the spring with strain sensor.

The final length of the assembled spring was 7 cm. Our sensor converts external weight into corresponding capacitance signals which can be used further to find the unknown weight of the object. So we have developed a low-power digital display system that shows the change in capacitance when the sensor is subjected to loading. Principle components of our system include a detection chip equipped with: sensors, microcontroller, bluetooth module, and software user interface. When our system is subjected to load, it acquires and transmits data via bluetooth communication and automatically shows the amount of detected force on the digital display. To display the practical applications of our sensor, we hanged our device with a small movable crane. When different loads are hanged on our device, the capacitance of the device increases linearly with the increase in load (Figure 4b). When the strain obtained from our system is compared with strain calculated from linear fitting, an error of less than 0.2% is observed. When the load is applied on the crane, our system displays the measured force, as shown in Figure 4c and Movie S1, Supporting Information. This demonstrates that the
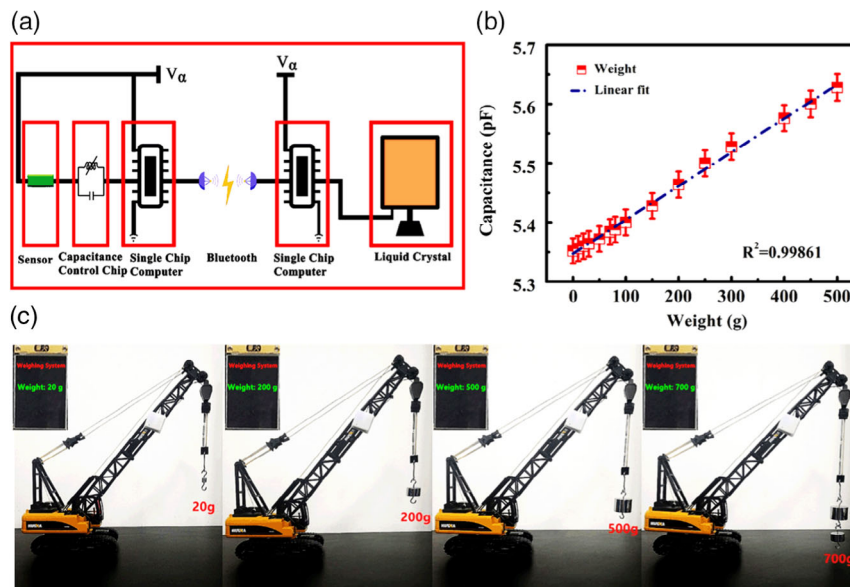

Figure 4. Application demo of adjustable modulus strain sensor. a) Block diagram showing the locally built low-power digital display system to display the amount of detected force during the loading of the sensor. For application demo, an assembled spring is attached with a sensor to attain wide-range force detection. b) Change in capacitance of the sensor as a function of the applied load. c) Real-time display of various detected loads on our digital display system.

**ADVANCED
SCIENCE NEWS**

www.advancedsciencenews.com

**ADVANCED
ENGINEERING
MATERIALS**

www.aem-journal.com

current sensor can be also used in monitoring the recovery of broken human joints, especially about the status of recovery, how much load can be carried, etc.

3. Conclusions

In this work, we presented a novel method of attaining an adjustable modulus strain sensor for wide-range force detection. The sensor consists of two LM filled TPE tubes encapsulated in flexible silicone. Various conventional springs are mounted with the strain sensor, and finally, springs' elastic coefficient-dependent modulus of the sensor is obtained in the range of 0.78–10.3 MPa. After optimizing the performance, a highly stretchable sensor capable of wide force-sensing range (0.07–74 N), high robustness (>3500 cycles), with low hysteresis, good linearity, and fast response time (<50 ms) is obtained. Finally, a local built strain-measuring system successfully measured the amount of detected force during the loading of the sensor, which confirms the great capability of the sensor to be applied in joint rehabilitation and soft robotic fields.

4. Experimental Section

Preparation of LM: Preparation of LM alloy Galinstan: High-purity metals gallium, indium, and tin (99.99%, Beijing Founde Star Sci. & Technol. Co., Ltd) were mixed together in the ratio of 68.2:21.8:10 by mass. Then the mixture was heated and stirred at 60 °C for 30 min under the nitrogen environment to obtain LM alloy galinstan ($Ga_{68.2}$ $In_{21.8}$ Sn_{10}). Galinstan is highly suitable for flexible soft sensors because it exhibits low modulus and very high conductivity even under large strain.[39–41]

Preparation of Capacitive Strain Sensor: TPE tubes used for device fabrication were bought from a local company (1.5 mm inner diameter). TPE exhibits high elasticity and is highly suitable for making stretchable sensors.[42,43] The core of the TPE was filled with galinstan, and copper rods were inserted at the end of each TPE tube which later on served as the source of electrical connection. Then the electrodes were encapsulated in a flexible silicone to form a stretchable capacitive strain sensor. To easily adjust the modulus of a strain sensor, springs of different elastic coefficients were mounted with the sensor. Fishing rope was installed on each spring to prevent its plastic deformation. Afterward, springs of different elastic coefficients were assembled by welding. Finally, the edges of the strain sensor with the help of a thin polyvinylidene fluoride plate sandwiched between two copper plates (fixed by elastic glue) were connected to the spring through a hole to form a complete strain sensor.

Characterization of the Microstructure: Microstructural examination of the sensor was conducted using an optical microscope (SteREO Discovery V12, ZEISS, Germany).

Measurements of Electrical Properties and Mechanical Properties: The capacitance measurements of the sensor were taken by LCR meter (IM 3570, HIOKI, Japan) at the oscillating frequency of 500 kHz. The mechanical properties were measured using a universal material testing machine (Instron 5943, USA). Tensile strain was measured by a locally developed tensile fatigue machine.

Supporting Information

Supporting Information is available from the Wiley Online Library or from the author.

Conflict of Interest

The authors declare no conflict of interest.

Keywords

[1] L. Federico, S. Enzo Pasquale, T. Mario, T. Alessandro, D. R. Danilo, *IEEE Trans. Inf. Technol. B* **2005**, *9*, 372.

[2] X. Yang, Z. Y. Zhou, F. Z. Zheng, M. Zhang, Y. G. Yao, in *TRANSDUCERS 2009-2009 Int. Solid-State Sensors, Actuators and Microsystems Conf.*, IEEE, Denver, CO, USA **2009**.

[3] S. S. Rautaray, A. Agrawal, in *2011 Int. Conf. on Multimedia, Signal Processing and Communication Technologies*, IEEE, Aligarh, India **2011**.

[4] J. Zhang, J. Liu, R. Zhuang, E. Mader, G. Heinrich, S. Gao, *Adv Mater.* **2011**, *23*, 3392.

[5] L. Cai, L. Song, P. Luan, Q. Zhang, N. Zhang, Q. Gao, D. Zhao, X. Zhang, M. Tu, F. Yang, W. Zhou, Q. Fan, J. Luo, W. Zhou, P. M. Ajayan, S. Xie, *Sci. Rep.* **2013**, *3*, 3048.

[6] C. Majidi, *Soft Robot.* **2014**, *1*, 5.

[7] Y. Wang, L. Wang, T. Yang, X. Li, X. Zang, M. Zhu, K. Wang, D. Wu, H. Zhu, *Adv. Funct. Mater.* **2014**, *24*, 4666.

[8] M. A. McEvoy, N. Correll, *Science* **2015**, *347*, 1261689.

[9] K. Takei, W. Honda, S. Harada, T. Arie, S. Akita, *Adv. Healthcare Mater.* **2015**, *4*, 487.

[10] S. Yao, P. Swetha, Y. Zhu, *Adv. Healthcare Mater.* **2018**, *7*, 1700889.

[11] S. Agarwala, G. L. Goh, T. S. Dinh Le, J. An, Z. K. Peh, W. Y. Yeong, Y. J. Kim, *ACS Sens.* **2019**, *4*, 218.

[12] L. M. Zhang, Y. He, S. Cheng, H. Sheng, K. Dai, W. J. Zheng, M. X. Wang, Z. S. Chen, Y. M. Chen, Z. Suo, *Small* **2019**, *15*, e1804651.

[13] H. Xu, Y. Lv, *Nanoscale* **2019**, *11*, 1570.

[14] J. Zhou, X. Xu, Y. Xin, G. Lubineau, *Adv. Funct. Mater.* **2018**, *28*, 1705591.

[15] H. Liu, M. Li, C. Ouyang, T. J. Lu, F. Li, F. Xu, *Small* **2018**, *14*, e1801711.

[16] Z. Liu, D. Qi, W. R. Leow, J. Yu, M. Xiloyannnis, L. Cappello, Y. Liu, B. Zhu, Y. Jiang, G. Chen, L. Masia, B. Liedberg, X. Chen, *Adv. Mater.* **2018**, *30*, e1707285.

[17] W. H. Choi, S. Kim, D. Lee, D. Shin, *IEEE Robot. Autom. Lett.* **2019**, *4*, 2539.

[18] C. Li, D. Wang, Y. Zhang, in *Int. Conf. on Universal Access in Human-Computer Interaction*, Springer, Berlin, Heidelberg **2007**.

**ADVANCED
SCIENCE NEWS**

www.advancedsciencenews.com

**ADVANCED
ENGINEERING
MATERIALS**

www.aem-journal.com

[19] A. G. Leal-Junior, A. Frizera, C. Marques, M. R. A. Sánchez, T. R. Botelho, M. V. Segatto, M. J. Pontes, *Opt. Fiber Technol.* **2018**, *41*, 205.

[20] S. Wagner, S. Bauer, *MRS Bull.* **2012**, *37*, 207.

[21] S. Pan, Z. Liu, M. Wang, Y. Jiang, Y. Luo, C. Wan, D. Qi, C. Wang, X. Ge, X. Chen, *Adv. Mater.* **2019**, *31*, e1903130.

[22] J. Duan, X. Liang, J. Guo, K. Zhu, L. Zhang, *Adv. Mater.* **2016**, *28*, 8037.

[23] D.-Y. Kang, H. Q. Jiang, Y. Huang, J. A. Rogers, *Science* **2014**, *311*, 208.

[24] S. H. Ha, M. B. Jeon, J. H. Cho, J. M. Kim, *Nanoscale* **2018**, *10*, 5105.

[25] J. T. Pham, J. Lawrence, Y. L. Dong, G. M. Grason, T. Emrick, A. J. Crosby, *Adv. Mater.* **2013**, *25*, 6635.

[26] J. T. Pham, J. Lawrence, G. M. Grason, T. Emrick, A. J. Crosby, *Phys. Chem. Chem. Phys.* **2014**, *16*, 10261.

[27] K. I. Jang, H. U. Chung, S. Xu, C. H. Lee, H. Luan, J. Jeong, H. Cheng, G.-T. Kim, S. Y. Han, J. W. Lee, *Nat. Commun.* **2015**, *6*, 6566.

[28] C. B. Cooper, I. D. Joshipura, D. P. Parekh, J. Norkett, R. Mailen, V. M. Miller, J. Genzer, *Sci. Adv.* **2019**, *5*, eaat4600.

[29] S. Xiang, T. Li, W. Dong, Q. Lu, *J. Polym. Sci., Polym. Phys.* **2018**, *56*, 1469.

[30] A. Maziz, A. Concas, A. Khaldi, J. Stalhand, N. K. Persson, E. W. Jager, *Sci. Adv.* **2017**, *3*, e1600327.

[31] G. Kharkova, O. Kononova, A. Krasnikovs, M. Eiduks, E. Machanovskis, K. Dzelzitis, in *Conf. Engineering for Rural Development*, International Scientific Con, Jelgava **2011**.

[32] J. Yang, W. Cheng, K. Kalantar-zadeh, *Proc. IEEE* **2019**, *107*, 2168.

[33] D. J. Lipomi, M. Vosgueritchian, B. C.-K. Tee, S. L. Hellstrom, J. A. Lee, C. H. Fox, Z. Bao, *Nat. Nanotechnol.* **2011**, *6*, 788.

[34] Y. Wang, S. Gong, S. J. Wang, X. Yang, Y. Ling, L. W. Yap, D. Dong, G. P. Simon, W. Cheng, *ACS Nano* **2018**, *12*, 9742.

[35] S. Gong, D. T. H. Lai, B. Su, K. J. Si, Z. Ma, L. W. Yap, P. Guo, W. Cheng, *Adv. Electron. Mater.* **2015**, *1*, 1400063.

[36] M.-Y. Cheng, C.-L. Lin, Y.-T. Lai, Y.-J. Yang, *Sensors* **2010**, *10*, 10211.

[37] T. Nakadegawa, H. Ishizuka, N. Miki, *Sens. Actuators, A* **2017**, *264*, 260.

[38] D.-J. Won, S. Baek, H. Kim, J. Kim, *Sens. Actuators, A* **2015**, *235*, 151.

[39] W. Qian, Y. Yang, L. Jing, *Adv. Eng. Mater.* **2017**, *20*, 1700781.

[40] M. D. Dickey, *Adv. Mater.* **2017**, *29*, 1606425.

[41] M. D. Bartlett, N. Kazem, M. J. Powell-Palm, X. Huang, W. Sun, J. A. Malen, C. Majidi, *Proc. Natl. Acad. Sci. U. S. A.* **2017**, *114*, 2143.

[42] S. Zhu, J. H. So, R. Mays, S. Desai, M. D. Dickey, *Adv. Funct. Mater.* **2013**, *23*, 2308.

[43] C. B. Cooper, K. Arutselvan, L. Ying, D. Armstrong, Y. Lin, M. R. Khan, J. Genzer, M. D. Dickey, *Adv. Funct. Mater.* **2017**, *27*, 1605630.